Cellular/Molecular

$GABA_B$ Receptor Modulation of Feedforward Inhibition through Hippocampal Neurogliaform Cells

Christopher J. Price,[1]* Ricardo Scott,[2]* Dmitri A. Rusakov,[2] and Marco Capogna[1]

[1]Medical Research Council Anatomical Neuropharmacology Unit, Oxford OX1 3TH, United Kingdom, and [2]Institute of Neurology, University College London, London WC1N 3BG, United Kingdom

Feedforward inhibition of neurons is a fundamental component of information flow control in the brain. We studied the roles played by neurogliaform cells (NGFCs) of stratum lacunosum moleculare of the hippocampus in providing feedforward inhibition to CA1 pyramidal cells. We recorded from synaptically coupled pairs of anatomically identified NGFCs and CA1 pyramidal cells and found that, strikingly, a single presynaptic action potential evoked a biphasic unitary IPSC (uIPSC), consisting of two distinct components mediated by $GABA_A$ and $GABA_B$ receptors. A $GABA_B$ receptor-mediated unitary response has not previously been observed in hippocampal excitatory neurons. The decay of the $GABA_A$ receptor-mediated response was slow (time constant = 50 ms), and was tightly regulated by presynaptic $GABA_B$ receptors. Surprisingly, the $GABA_B$ receptor ligands baclofen and (2*S*)-3-{[(1*S*)-1-(3,4-dichlorophenyl)ethyl]amino-2-hydroxypropyl}(phenylmethyl)phosphinic acid (CGP55845), while affecting the NGFC-mediated uIPSCs, had no effect on action potential-evoked presynaptic Ca^{2+} signals monitored in individual axonal boutons of NGFCs with two-photon microscopy. In contrast, baclofen clearly depressed presynaptic Ca^{2+} transients in non-NGF interneurons. Changes in extracellular Ca^{2+} concentration that mimicked the effects of baclofen or CGP55845 on uIPSCs significantly altered presynaptic Ca^{2+} transients. Electrophysiological data suggest that $GABA_B$ receptors expressed by NGFCs contribute to the dynamic control of the excitatory input to CA1 pyramidal neurons from the temporoammonic path. The NGFC–CA1 pyramidal cell connection therefore provides a unique and subtle mechanism to shape the integration time domain for signals arriving via a major excitatory input to CA1 pyramidal cells.

Key words: **interneuron; synaptic transmission; $GABA_B$ receptor; temporoammonic path; Ca^{2+} imaging; feedforward inhibition**

Introduction

In feedforward inhibitory circuits, the afferent fibers directly excite an inhibitory cell, which in turn inhibits the firing of the target neuron. Feedforward inhibition is widespread in the brain because it maintains timing of spiking across different cell populations, by limiting the temporal summation of excitatory inputs (Buzsáki, 1984; Turner, 1990; Pouille and Scanziani, 2001; Blitz and Regehr, 2005; Gabernet et al., 2005; Mittmann et al., 2005). Axon terminals of feedforward inhibitory neurons usually express presynaptic receptors, such as $GABA_B$ receptors (Thompson et al., 1993; Vigot et al., 2006). However, elucidating the role of these receptors is often problematic, mainly because similar receptors could also be expressed in other presynaptic or postsynaptic locations throughout the circuit.

The temporoammonic (TA) path (also known as perforant path) connects the entorhinal cortex and the CA1 area of hippocampus and is equipped with a feedforward inhibitory circuit. The TA path fibers form excitatory synapses on CA1 pyramidal cells (Witter et al., 1988; Yeckel and Berger, 1990; Colbert and Levy, 1992; Yeckel and Berger, 1995; Gloveli et al., 1997) and also monosynaptically activate interneurons with the soma in the stratum lacunosum moleculare (SLM), which in turn project to CA1 pyramidal cells (Williams et al., 1994; Empson and Heinemann, 1995a,b; Remondes and Schuman, 2002). Interneurons of SLM are a heterogeneous population (Freund and Buzsáki, 1996; McBain and Fisahn, 2001; Maccaferri and Lacaille, 2003; Somogyi and Klausberger, 2005). Previously, we described a network of so-called neurogliaform cells (NGFCs), with the soma, dendrites, and much of their axon in the SLM (Price et al., 2005). Unitary inhibitory synaptic responses recorded from connected NGFC–NGFC pairs show pronounced short-term depression and a slow decay, and, uniquely, are mediated by both $GABA_A$ and $GABA_B$ receptors (Price et al., 2005). This is consistent with the properties of synapses formed by NGFCs in the neocortex (Tamás et al., 2003; Szabadics et al., 2007).

Virtually all we know to date about synapses formed by hippocampal NGFCs comes from recordings in postsynaptic NGFCs. However, NGFCs frequently target pyramidal cells (Vida et al., 1998). Therefore, it is important to ascertain whether the slow $GABA_A$ and $GABA_B$ receptor-mediated responses characteristic for NGFC pairs can also be detected in the NGFC–pyramidal cell synapse. This would identify one cell type responsible for the slow $GABA_A$ receptor-mediated responses recorded in CA1 pyramidal cells (Pearce, 1993), and also establish similarities with the NGFC

Received April 13, 2007; revised April 22, 2008; accepted May 15, 2008.

This work was supported by the Medical Research Council, United Kingdom, Wellcome Trust, European Union (Promemoria), and Human Frontier Science Program. We thank Dr. Raffaella Geracitano, David Elfant, Theofanis Karayannis, and Tatjana Lalic for comments on a previous version of this manuscript. We acknowledge Romana Hauer and Ben Micklem for their technical aid and expertise.

*C.J.P. and R.S. contributed equally to this work.

Correspondence should be addressed to Dr. Marco Capogna, Medical Research Council Anatomical Neuropharmacology Unit, Mansfield Road, Oxford OX1 3TH, UK. E-mail: marco.capogna@pharm.ox.ac.uk.

C. J. Price's present address: Department of Physiology, Queens University, Kingston, Ontario, Canada K7L 3N6.

DOI:10.1523/JNEUROSCI.4673-07.2008

 0270-6474/08/286974-09$15.00/0

circuitry of the neocortex (Tamás et al., 2003; Szabadics et al., 2007). Furthermore, the TA path–CA1 circuitry offers a chance to study the role of $GABA_B$ receptors expressed by interneurons of a feedforward circuit, because the TA path fibers are insensitive to $GABA_B$ receptor ligands under normal conditions (Ault and Nadler, 1982; Colbert and Levy, 1992), unlike other excitatory fibers (Thompson et al., 1993).

We therefore used paired recordings and two-photon microscopy to establish the main characteristics of NGFC–CA1 pyramidal cell synapses, and the modulatory role of $GABA_B$ receptors in providing feedforward regulation of the TA path input to the hippocampal circuitry.

Materials and Methods

Slice preparation. All procedures involving animals were performed using methods approved by the United Kingdom Home Office and according to The Animals (Scientific Procedures) Act (1986). Juvenile CD rats (Charles River) between 18 and 24 d old were anesthetized with isoflurane and decapitated. The brain was quickly removed, extra tissue was trimmed away, and the remaining block containing the hippocampus was mounted for vibratome sectioning in ice-cold artificial CSF (ACSF) containing the following (in mM): 130 NaCl, 3.5 KCl, 2.5 $CaCl_2$, 1.5 $MgSO_4$, 1.25 NaH_2PO_4, 24 $NaHCO_3$, and 10 glucose and saturated with 95% O_2 and 5% CO_2, to which was added 3 mM kynurenic acid. Horizontal sections (thickness: 300–320 μm) were prepared consisting of the dorsal hippocampus and attached entorhinal cortex, which were allowed to recover in ACSF without kynurenic acid first at 35 ± 2°C for ~15 min and then at room temperature for at least 45 min before recording. Alternatively, a high-sucrose/high-magnesium solution containing the following (in mM): 87 NaCl, 25 $NaHCO_3$, 25 glucose, 75 sucrose, 2.5 KCl, 1.25 NaH_2PO_4, 0.5 $CaCl_2$, and 7 $MgCl_2$ was also used for slice preparation.

Electrophysiology. Single and paired whole-cell recordings were performed using an EPC9/2 amplifier (HEKA). Slices were placed in a recording chamber and were constantly superfused with ACSF and maintained at a temperature of 33 ± 2°C. The NGFCs in the CA1 SLM were visually identified based on soma shape and size. Recording electrodes were filled with either of the following (in mM): 126 K-gluconate, 10 HEPES, 10 Na_2-phosphocreatine, 4 KCl, 4 Mg-ATP, 0.3 Na-GTP, and 0.5% biocytin (pH 7.3 with KOH); or 126 Cs-methanesulfonate, 4 CsCl, 10 HEPES, 10 Na_2-phosphocreatine, 4 Mg-ATP, 0.3 Na-GTP, and 0.5% biocytin (pH 7.3 with CsOH). Patch pipettes had resistances between 3 and 7 MΩ. For Ca^{2+}-imaging experiments, the internal solution included the following (in mM): 135 K-methanesulfonate, 2 $MgCl_2$, 10 HEPES, 10 Na-phosphocreatine, 4 Na-ATP, 0.4 Na-GTP, 0.5% biocytin, and the fluorescence indicators (pH 7.3 with KOH). Series resistance was compensated by 60–70%, and the experiments discontinued if it increased >20% throughout the recording period. An empirically determined liquid junction potential of −12 mV was added to the calculation of the resting membrane potential for the current-clamp experiments. Synaptic potentials and currents were evoked in CA1 pyramidal cells after stimulation of the TA pathway using a concentric bipolar electrode (25 μm platinum iridium tip; FHC) inserted close to the presubiculum. In these experiments, to avoid possible recruitment of the hippocampal trisynaptic pathway, the CA3 region of the hippocampus was dissected away, leaving the entorhinal cortex, dentate gyrus, CA1, and subiculum (Empson and Heinemann, 1995b). However, we cannot rule out the possibility that signals may have also arisen from fibers that originated in the thalamic nucleus reunions, amygdala, or inferotemporal cortex that send axons to the SLM (Amaral and Witter, 1995). The stimulation of Schaffer collaterals was also obtained via a concentric bipolar electrode. Patch pipettes filled with oxygenated ACSF were used for extracellular recordings.

Electrophysiological data were analyzed off-line using Pulsefit (HEKA) and IGOR Pro 5 (WaveMetrics). The peak amplitude of the early $GABA_A$ receptor-mediated synaptic currents was calculated from the average of the five maximum values within a time window between 15 and 45 ms from the peak of the presynaptic action current in an average trace of five sweeps. The same applied for the calculation of the late $GABA_B$ receptor-mediated synaptic currents, but in this case the time window to obtain the peak was between 150 and 225 ms from the peak of the presynaptic action current. Statistical tests used are indicated throughout the text and were performed by using PRISM (GraphPad) or SPSS. Unless indicated otherwise, values presented in the text and in figures represent the mean ± SEM.

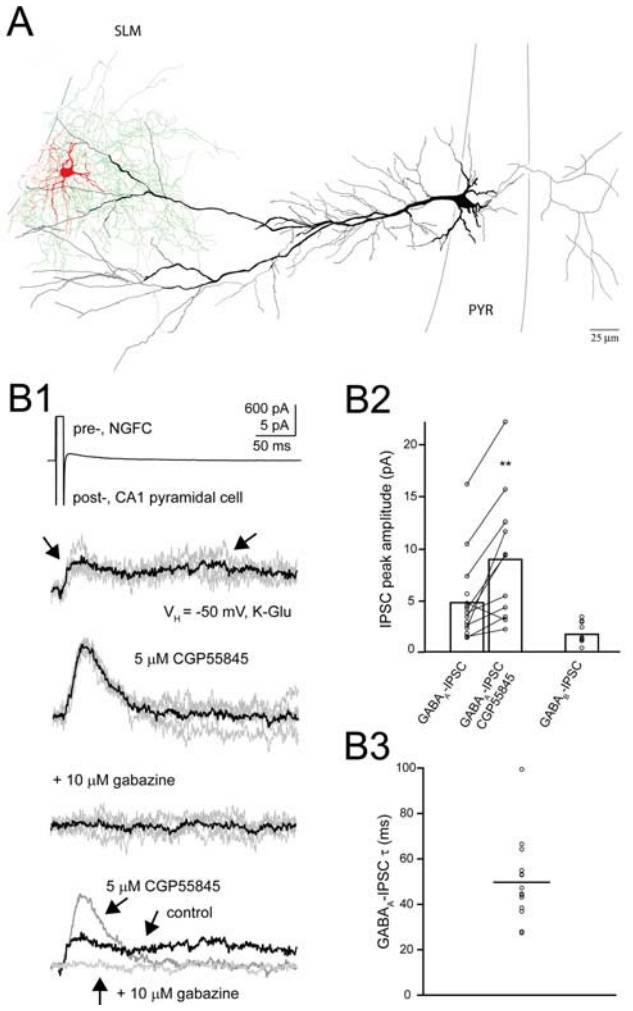

Figure 1. Postsynaptic $GABA_A$ and $GABA_B$ receptors mediated uIPSCs in NGFC–CA1 pyramidal cell pair recordings. ***A***, Light microscopic reconstruction of a biocytin-labeled NGFC of SLM (soma and dendrites in red, axon in green) and a postsynaptic CA1 pyramidal cell (soma, dendrites, and truncated axon in black). Note that the axonal arbor of the NGFC remains segregated within the SLM, where it overlaps with the distal dendritic arborization of the CA1 pyramidal cell. PYR, Pyramidal cell layer. ***B1***, Voltage-clamp recording between the NGFC and the CA1 pyramidal cell pair shown above. The arrows denote the early and late uIPSCs. Note that the $GABA_B$ receptor antagonist CGP55845 (5 μM) increased the early peak amplitude of the uIPSC and abolished the late component of the uIPSC. Subsequently the $GABA_A$ receptor antagonist gabazine (10 μM) abolished the residual synaptic current. From top to bottom: presynaptic action current; postsynaptic uIPSCs in control, in the presence of CGP55845, and after addition of gabazine (for each group of traces: black trace, average; gray traces, five single sweeps); and average traces illustrated above superimposed. ***B2***, Histograms representing the mean peak amplitude of the early and late uIPSCs; open circles represent individual data points. The $GABA_B$ receptor antagonist CGP55845 increased the peak amplitude of the early $GABA_A$-IPSC (**$p < 0.01$; $n = 11$; paired t test). ***B3***, Summary graph illustrating the mean and the decay time constants fitted from the uIPSCs of various NGFC–CA1 pyramidal cell pairs ($n = 14$); open circles represent individual data points. Whole-cell patch-clamp recording was performed with K-gluconate-based intracellular solution; V_H of the postsynaptic neurons was −50 mV.

Ca^{2+} imaging. Imaging experiments were performed using a multiphoton excitation setup comprising a Radiance 2000 imaging system (Zeiss–Bio-Rad) optically linked to a femtosecond laser MaiTai (SpectraPhysics) and integrated with a single-cell electrophysiology rig (Rusa-

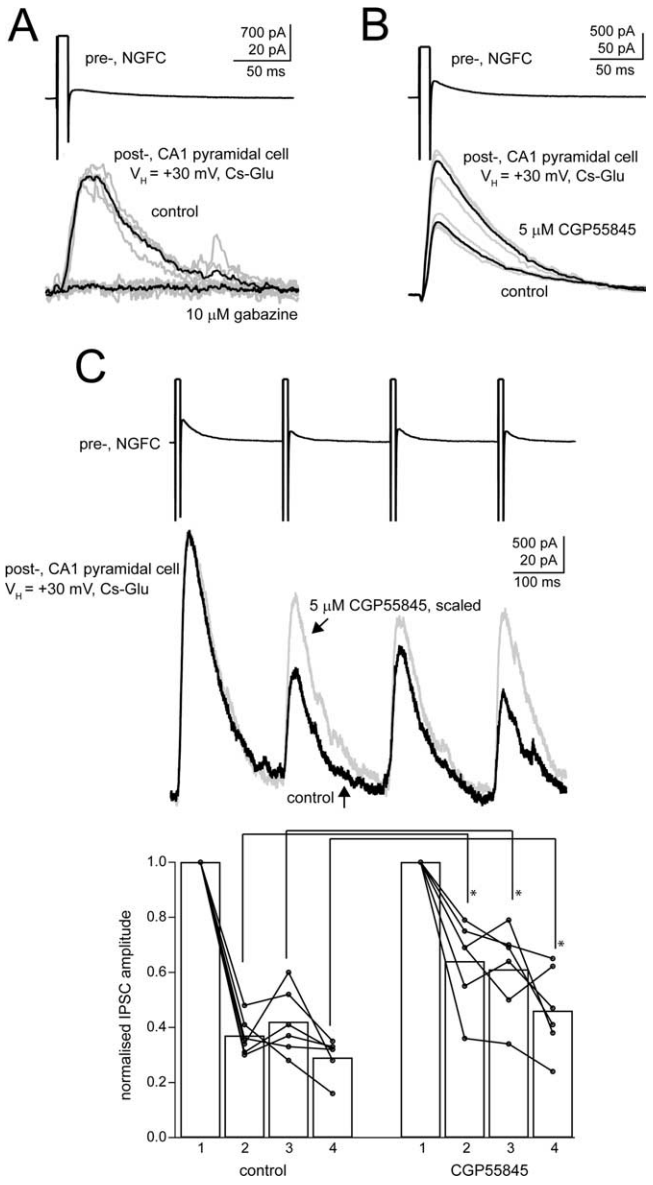

Figure 2. Further features of $GABA_B$ receptor-mediated involvement in uIPSCs of NGFC–CA1 pyramidal cell pairs. ***A***, Action currents in a presynaptic NGFC (top trace) evoked uIPSCs abolished by the $GABA_A$ receptor gabazine (10 μM) in a postsynaptic neuron recorded with cesium-based patch pipette (bottom traces). ***B***, In another cell pair, under the same experimental conditions as in ***A***, the $GABA_B$ antagonist CGP55845 (5 μM) increased the size of the uIPSCs. Black traces, Average; gray traces, single sweeps (5 in ***A***, 3 in ***B***), shown superimposed. ***C***, Voltage-clamp recordings (top trace, presynaptic action currents; bottom traces superimposed, average of three sweeps of postsynaptic uIPSCs in control in the presence of CGP55845) from an NGFC–CA1 pyramidal cell pair showing that 5 μM CGP55845 inhibits the depression observed with 5 Hz stimulation. Note that the trace in the presence of CGP55845 is scaled to the control trace, and that the calibration bar refers to the control trace. The histograms, on the bottom, represent the amplitude of each of the four IPSCs (1–4) recorded during 5 Hz train stimulation under control and 5 μM CGP55845 conditions normalized to the amplitude of the first IPSC. The depression was reduced by CGP55845 (*$p < 0.05$; $n = 6$; paired t test). Data from individual cells are also illustrated (circles). Whole-cell patch-clamp recording was performed with cesium-based intracellular solution; V_H of the postsynaptic neurons was +30 mV.

kov and Fine, 2003). NGFCs were held in whole-cell mode and loaded with two fluorescent indicators, a morphological tracer (Alexa Fluor 594; 20 μM), and a Ca^{2+}-sensitive dye (Fluo-4; 200 μM). Fluorophores were excited in two-photon mode at 810 nm, with the laser power optimized for emission detection at different depths in the slice. The axon was identified and traced from one of the dendrites using frame-scanning mode (256 × 256 pixels, 500 Hz; the number of frames taken was kept small to minimize phototoxic damage), and the system was focused at the maximum optical resolution (~0.2 μm; digital capture, 70 nm per pixel) on varicosities showing prominent action potential-evoked Ca^{2+} influx (in contrast to dendritic compartments, which invariably showed either smaller or undetectable action potential-evoked Ca^{2+} transients; see Results). We started the recording when the resting fluorescence in both Alexa and Fluo-4 channels was stable (~1–2 h after break-in). Action potentials were routinely evoked by 2 ms somatic command voltage pulses. Fluorescence transients were recorded in linescan mode at 500 Hz (500 ms sweeps; intersweep interval, 2 min), and stored for off-line analysis. The Ca^{2+}-dependent fluorescence response $\Delta F/F$ (integrated over the visible varicosity width) was calculated as $(F_{post} - F_{pre})/(F_{pre} - F_0)$. The values of F_{pre} and F_{post} represent the linescan fluorescence averaged over, respectively, 100 ms before the first spike and 50 ms after each spike onset in the case of fluorescent transients in response to a single pulse or 5 Hz four-pulse trains. F_0 denotes the background fluorescence measured outside any structure filled with the indicator. In the case of five-response amplitude measurements (20 Hz train of five action potentials), the fluorescence signal for each pulse was averaged over 25 ms after each spike onset. Brief trains at 20 Hz, as opposed to single stimuli, were applied to increase the release of GABA and thus boost the activation of presynaptic $GABA_B$ receptors. We also analyzed Ca^{2+} signals in response to both the first and all five action potentials during the train, the latter to optimize the signal-to-noise ratio. Paired-pulse ratios (PPRs) were obtained by dividing the amplitude (averaged over 50 ms after spike) of the nth fluorescence transient by the amplitude of the first transient in the train. Image analyses were performed on stacks of stored linescan images using a set of custom NIH Image macros. False color tables and averaged images were used for illustration purposes, but the original (gray level) pixel brightness values in each linescan image were used for the quantitative analysis. In most experiments, we reconstructed the axon trajectory using a collage of high-resolution Kalman-filtered z-stacks 15–20 μm deep. A more detailed description of axonal imaging was previously published (Scott and Rusakov, 2006).

Cell reconstruction and immunocytochemistry. To verify the identity of recorded neurons, in both the electrophysiological and imaging experiments, neurons were filled with biocytin and processed to reveal their dendritic and axonal patterns. After recording, cells were immediately fixed for at least 24 h by immersion in 4% paraformaldehyde and 15% saturated (v/v) picric acid (~0.2%) in 0.1 M phosphate buffer (pH 7.4). Slices were resectioned using a vibratome at 60 μm after being embedded in gelatin. Biocytin was then visualized with diaminobenzidine using the Vector ABC kit (Vector Laboratories) and intensified with osmium tetroxide. Neurons were later drawn at 63× (dendrites) and 100× (axons) using a drawing tube.

Chemicals and drugs. All drugs were applied to the recording preparation through the bath. Salts used in the preparation of the internal recording solution and ACSF were obtained from either BDH Laboratory Supplies or Sigma. 6,7-Dinitroquinoxaline-2,3-dione (DNQX), SR95531 (gabazine throughout the text), (2*S*)-3-{[(1*S*)-1-(3,4-dichlorophenyl)-ethyl]amino-2-hydroxypropyl}(phenylmethyl)phosphinic acid (CGP55845), and baclofen came from Tocris Bioscience.

Results

We recorded from synaptically connected pairs of neurons identified *post hoc* as NGFCs (presynaptic) and CA1 pyramidal cells (postsynaptic) (Fig. 1*A*). NGFCs were characterized by a round cell body, short and aspiny dendrites that emerged in a stellate manner and remained close to the soma, and an axon that branched profusely close to the soma, producing a dense arbor that is a hallmark of this cell type. The axon of NGFCs targeted only the distal portion of the apical dendrites of CA1 pyramidal cells (Fig. 1*A*). A single action potential (escape action current) in a presynaptic NGFC evoked a unitary IPSC (uIPSC) in the postsynaptic pyramidal cell (Figs. 1*B*, 2). The uIPSCs had several unique features. First, they showed unusual biphasic kinetics with an early peak of 4.9 ± 1 pA at 29 ± 14 ms ($n = 15$) and a late

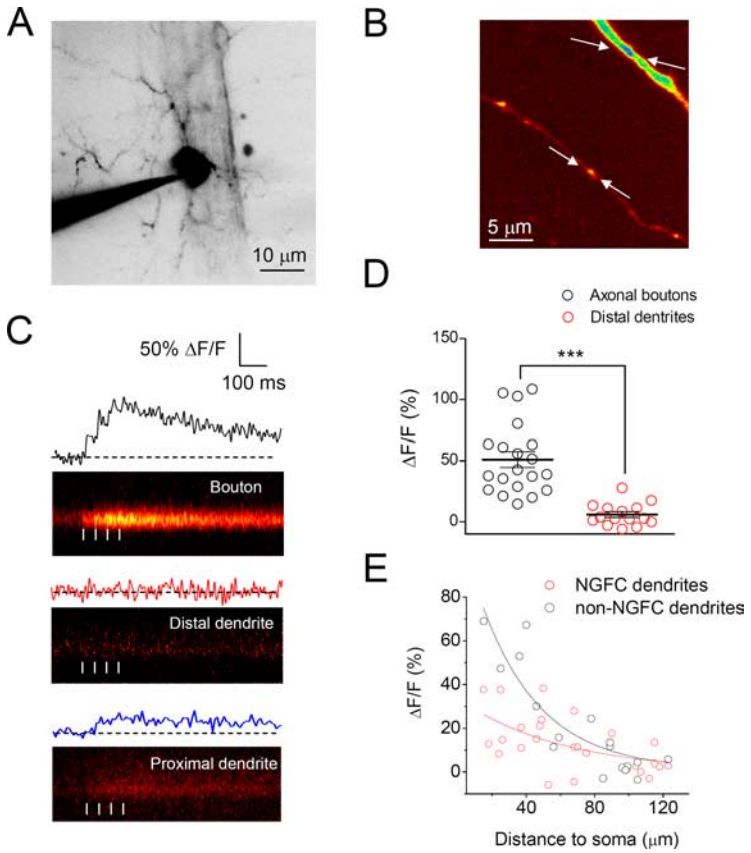

Figure 3. Ca^{2+} signals in axons and dendrites of hippocampal NGFCs elicited by action potentials. ***A***, Characteristic image of an NGFC (Alexa Fluor 594 channel) occurring near a blood capillary (vertical shadow). ***B***, Fragments of an axon (bottom) and an aspiny dendrite (top) imaged in the same cell; arrows indicate linescan positioning (see below). ***C***, Ca^{2+}-dependent fluorescence signals evoked by four actions potentials (ticks) in the axonal varicosity (top; shown in ***B***), at a distal dendritic site (middle; shown in ***B***), and at a proximal dendrite (~25 μm from the soma; not shown). ***D***, The amplitude of action potential-evoked Ca^{2+} transients is much larger at the axonal varicosities ($n = 20$) than at dendritic sites ($n = 15$; ***$p < 0.001$; unpaired *t* test). Average, SEM, and individual data points (circles) are illustrated. ***E***, The amplitude of dendritic Ca^{2+} signals in NGFCs (red) and non-NGF interneurons (black) decreases with the distance from the soma; lines, monoexponential fit.

peak of 1.9 ± 0.3 pA at 187 ± 44 ms ($n = 11$ of 15 cells) at V_H of −50 ± 2 mV recorded with a K-gluconate-filled patch pipette (Fig. 1*B1*,*B2*). The early and late components of uIPSCs were abolished by, respectively, the $GABA_A$ and $GABA_B$ receptor-specific antagonists gabazine (10 μM; $n = 15$) and CGP55845 (5 μM; $n = 11$) in all cells tested (Fig. 1*B1*). Furthermore, the early component was enhanced by CGP55845 (see below). When postsynaptic CA1 pyramidal neurons were recorded with cesium-containing patch pipettes, to block postsynaptic $GABA_B$ receptors (Gähwiler and Brown, 1985), the late uIPSC component was abolished, and the uIPSCs were entirely blocked by gabazine (10 μM; $n = 8$; $V_H = +30$ mV to enhance the driving force for Cl^-) (Fig. 2*A*). This further indicated that the late and the early components were mediated by $GABA_B$ and $GABA_A$ receptors, respectively. Second, the decay of the $GABA_A$ receptor component of the uIPSCs was slow and well fitted with a single exponential (time constant, 50 ± 4.9 ms; $n = 14$), when measured in the presence of 5 μM CGP55845 (Fig. 1*B3*). Third, the peak amplitude of the $GABA_A$ receptor-mediated current was significantly enhanced by 5 μM CGP55845 (to 169 ± 17% of control; $p < 0.01$; $n = 11$; paired *t* test) (Fig. 1*B1*,*B2*), indicating tonic activation of $GABA_B$ receptors in control conditions. This effect could be reproduced with cesium-containing patch pipettes ($V_H = +30$ mV), consistent with the involvement of presynaptic $GABA_B$ receptors (Fig. 2*B*). On average, the uIPSC peak amplitude was enhanced to 139 ± 18% of control by 5 μM CGP55845 under these conditions ($p < 0.05$; $n = 7$; paired *t* test). Fourth, the stimulation of presynaptic NGFCs at 5 Hz (intersweep interval, 2 min), to mimic theta frequency range, elicited strong depression of the uIPSCs recorded from CA1 pyramidal cells with cesium-containing patch pipettes at V_H of + 30 mV. This short-term depression was significantly inhibited by 5 μM CGP55845 ($p < 0.05$; $n = 6$; paired *t* test) (Fig. 2*C*), consistent with a phasic activation by presynaptic $GABA_B$ receptors.

In summary, action potentials generated by NGFCs induced uIPSCs in CA1 pyramidal cells consisting of distinct $GABA_A$ and $GABA_B$ receptor-mediated components. The $GABA_A$ receptor-mediated component had a slow decay and displayed use-dependent depression during theta frequency stimulation. Endogenous tonic and phasic activation of presynaptic $GABA_B$ receptors regulates the strength of transmission at these synapses.

Inhibitory action of presynaptic $GABA_B$ receptors in NGFCs does not rely on presynaptic Ca^{2+}

Do presynaptic $GABA_B$ receptors of NGFCs act through changes in presynaptic Ca^{2+} signaling? Because presynaptic voltage-dependent Ca^{2+} channels are the classical targets of $GABA_B$ receptors (Takahashi et al., 1998), they represent an obvious candidate. However, $GABA_B$ receptors have also been demonstrated to target directly components of the exocytotic release machinery (Sakaba and Neher, 2003), consistent with earlier suggestions (Thompson et al., 1993). To establish whether changes in presynaptic Ca^{2+} could explain the action of presynaptic $GABA_B$ receptors in NGFCs, we monitored Ca^{2+} transients evoked by action potentials at individual axonal boutons of NGFCs identified in CA1 SLM using a set of criteria established previously (Rusakov et al., 2004). To carry out linescan recordings at selected boutons, we loaded the neurons with the morphological tracer Alexa Fluor 594 for >1 h, a time when we still observed short-term synaptic depression in the paired recording experiments. This protocol allowed visualization of the dense axonal plexus of NGFCs (Kalman average images of two different cells are shown in Figs. 3*A* and 6*A*). We also confirmed the cell identity *post hoc* using immunodetection with biocytin. The axons were usually 3–5 times thinner than proximal dendrites (Fig. 3*B*). We found that although action potentials elicited large Ca^{2+} transients at axonal varicosities, dendrites of the same cells showed either smaller or undetectable Ca^{2+} responses (Fig. 3*C*,*D*). This observation was useful in cross-validating the axonal identity in NGFCs. The magnitude of action potential-evoked dendritic Ca^{2+} transients was inversely correlated with the distance of the soma in both NGFCs and non-NGFCs of SLM (Fig.

3*E*), consistent with previous results in other types of interneurons (Goldberg et al., 2003).

Four action potentials at 5 Hz, the protocol used in paired recording experiments, evoked clear Ca^{2+}-dependent fluorescent transients at axonal varicosities (Fig. 4). Surprisingly, the $GABA_B$ receptor antagonist CGP55845 (5 μM), which significantly enhanced the IPSCs during the train, had no detectable effect on presynaptic Ca^{2+} transients evoked by any action potential in the train (Fig. 4*B*) ($p > 0.5$ for each comparison; $n = 19$; paired *t* test), or on the ratios of the Ca^{2+} signals elicited by the second, third, or fourth versus the first action potential (Fig. 4*C*) ($p > 0.6$ for each comparison; $n = 19$; paired *t* test). Even when Ca^{2+} transients were evoked by a brief train of action potentials at 20 Hz, to enhance the release of GABA, CGP55845 had no significant effect (supplemental Fig. 1*A*, available at www.jneurosci.org as supplemental material) ($p > 0.7$; $n = 7$; paired *t* test). The application of the $GABA_B$ receptor agonist baclofen (10 μM), which reversibly depressed the uIPSC elicited by a single presynaptic action potential (Fig. 5*A*,*C*) (14.1 ± 2% of control; $p < 0.05$; $n = 4$; paired *t* test), had no detectable effect on single action potential-evoked presynaptic Ca^{2+} transients either (Fig. 6*B*,*C*) ($p > 0.7$; $n = 9$; paired *t* test). Likewise, although baclofen (10 μM) depressed the uIPSCs elicited by a train of action potentials (supplemental Fig. 2*A*, available at www.jneurosci.org as supplemental material) ($p < 0.05$; $n = 4$; paired *t* test), it did not affect presynaptic Ca^{2+} events in response to a train of stimuli (supplemental Fig. 1*B*, available at www.jneurosci.org as supplemental material) ($p > 0.7$; $n = 10$; paired *t* test). In contrast, in similar recordings performed in non-NGF interneurons with the soma in the SLM, baclofen (10 μM) decreased (to 49 ± 19% of baseline) presynaptic Ca^{2+} transients elicited by a single presynaptic action potential (supplemental Fig. 1*C*, available at www.jneurosci.org as supplemental material) ($p < 0.05$; $n = 9$; paired *t* test) or by a train of action potentials (supplemental Fig. 1*C*, available at www.jneurosci.org as supplemental material) ($p < 0.001$; $n = 9$; paired *t* test).

To further validate the sensitivity of our imaging experiments, we raised the extracellular Ca^{2+} concentration from 2.5 to 3.5 mM. This increased the amplitude of the uIPSCs to an extent similar to that of CGP55845 (Fig. 5*B*,*C*) (145.1 ± 6.5% of control; $p < 0.05$; $n = 4$; paired *t* test), but also enhanced action potential-evoked presynaptic Ca^{2+} transients (Fig. 6*D*,*E*) (45 ± 15% of control; $p < 0.01$; $n = 13$; ANOVA). Conversely, decreasing the extracellular Ca^{2+} concentration from 2.5 to 1 mM reproduced the inhibitory effect of baclofen on the uIPSCs (Fig. 5*B*,*C*) (14.2 ± 0.9% of control; $p < 0.05$; $n = 4$; ANOVA), and also decreased the presynaptic Ca^{2+} transient (Fig. 6*D*,*E*) (70 ± 6% of control; $p < 0.01$; $n = 10$; ANOVA). The uIPSCs and Ca^{2+} transients elicited by trains of action potentials were also significantly affected by changes in extracellular Ca^{2+} concentrations (uIPSCs: $p < 0.05$; $n = 4$; ANOVA; Ca^{2+} events: $p < 0.01$; ANOVA; $n = 10$) (supplemental Figs. 2*B*, 3*A*,*B*, available at www.jneurosci.org as supplemental material). Finally, the application of 100 μM $CdCl_2$ abolished presynaptic Ca^{2+} transients ($n = 3$) (supplemental Fig. 3*C*, available at www.jneurosci.org as supplemental material), confirming the involvement of voltage-gated Ca^{2+} channels. These results indicated that presynaptic $GABA_B$ receptor-mediated modulation of the NGFC–CA1 pyramidal cell transmission could not be explained by the changes in presynaptic Ca^{2+} signaling, suggesting the likelihood for the presynaptic release machinery to be directly affected.

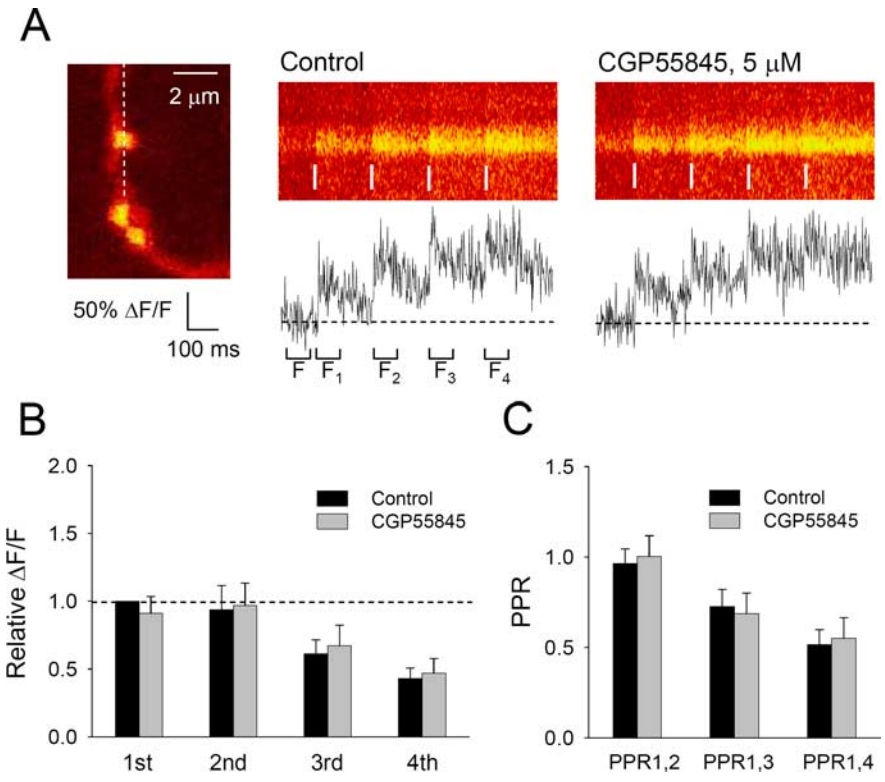

Figure 4. $GABA_B$ receptors have no detectable effect on presynaptic Ca^{2+} signaling in NGFC axons. ***A***, Effect of bath-applied CGP55845 (5 μm) on presynaptic Ca^{2+} transients (linescans and traces) evoked by four action potentials at 5 Hz at the axonal varicosity shown in the left panel. The fluorescence measurement intervals are indicated. ***B***, Pooled data: CGP55845 had no detectable effect on fluorescence transients induced by individual action potentials in a 5 Hz train ($p > 0.5$ for all the peaks; paired *t* test; $n = 19$). The apparent use-dependent reduction of fluorescence responses is likely to reflect progressive changes in endogenous buffer and/or Ca^{2+} indicator saturation. ***C***, Effect of CGP55845 on PPR for all fluorescence peaks during the train with respect to the first transient (nonsignificant with $p > 0.6$ for each comparison; paired *t* test; $n = 19$).

$GABA_B$ receptors expressed by NGFCs dynamically modulate TA path–CA1 EPSPs

What is the physiological role of the $GABA_B$ receptors expressed by NGFCs? The monosynaptic NGFC–CA1 pyramidal cell connection is ideally positioned to influence the integration by a pyramidal cell of the TA path input (Price et al., 2005). We expect that synaptic inhibition dynamically controls the duration of excitatory responses (Gabernet et al., 2005), and that $GABA_B$ receptors expressed at NGFC axon terminals tightly regulate this control. The $GABA_B$ receptors are not expressed at the TA path–CA1 pyramidal cell synapses under normal conditions (Ault and Nadler, 1982; Colbert and Levy, 1992). We confirmed this lack of sensitivity under our experimental conditions: 20 μM baclofen had no effect on either the amplitude or the slope of the field EPSPs recorded in the CA1 area in response to 0.1 Hz stimulation of TA path (99 ± 1% of control values for both parameters; $n = 3$) (Fig. 7*A*) but reversibly abolished the population spike evoked

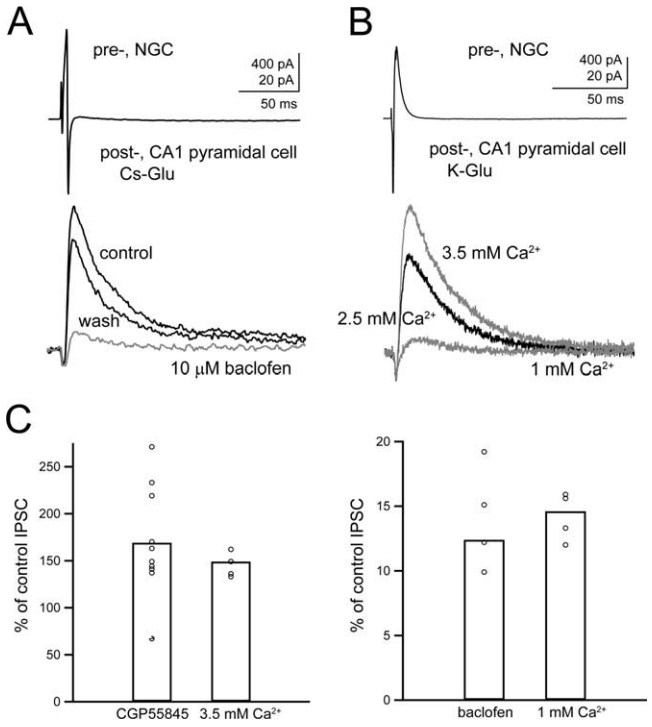

Figure 5. Raising or decreasing $[Ca^{2+}]_o$ or the application of $GABA_B$ receptor ligands affect uIPSCs. ***A***, Action currents in a presynaptic NGFC (top trace) evoked uIPSCs (bottom traces), which were reduced by the $GABA_B$ agonist baclofen (10 μM) in a reversible manner. ***B***, In another cell pair, the amplitude of the uIPSCs was changed by decreasing or increasing $[Ca^{2+}]_o$ to 1 and 3.5 mM, respectively. The postsynaptic neurons were recorded at $V_H = -50$ mV with Cs-gluconate- (***A***) or K-gluconate- (***B***) based patch pipettes. ***C***, Left graph, The histograms show the effects of CGP55845 (5 μM) and 3.5 mM extracellular Ca^{2+} on the uIPSCs normalized to control. Both agents increased the uIPSCs ($p < 0.05$; paired-*t* test; $n = 10$ and 4, respectively) to a similar extent ($p > 0.05$; unpaired *t* test). ***C***, Right graph, The histograms illustrate the effects of baclofen and 1 mM extracellular Ca^{2+} on the uIPSCs normalized to control. Both agents decreased the uIPSCs ($p < 0.05$; paired-*t* test; $n = 4$ for both) to a similar extent ($p > 0.05$; unpaired *t* test). Each value represents a single experiment.

by 0.1 Hz stimulation of Schaffer collaterals (Fig. 7*B*) ($n = 3$; these experiments were performed in the presence of 0.3–1 μM gabazine to block $GABA_A$ receptors).

Therefore, any presynaptic effect of $GABA_B$ ligands on postsynaptic responses evoked in CA1 pyramidal cells by TA path stimulation is most likely to require $GABA_B$ receptors on inhibitory interneurons. We therefore examined the effect of the $GABA_B$ receptor antagonist CGP55845 (5 μM) on the EPSP–IPSP sequence elicited in CA1 pyramidal cells by the TA path stimulation, with $GABA_A$ receptors left intact. The cells were recorded with cesium-containing patch pipettes at the resting membrane potentials, i.e., between the reversal potentials for excitatory and IPSPs. The stimulation of the TA path with four stimuli at 5 Hz every 1 min evoked EPSP–IPSP sequences in CA1 pyramidal cells (response to the first stimulus is cited as EPSP1, to the second stimulus as EPSP2, and so on). In control, we observed a marked increase in the half-peak duration and amplitude of the EPSPs occurring after the first stimulus within the train ($p < 0.05$, ANOVA, for EPSP1 vs EPSP2, EPSP3, or EPSP4; $n = 5$), and a steady decrease in the amplitude of the IPSPs ($p < 0.05$, ANOVA, for IPSP1 vs IPSP2, IPSP3, or IPSP4; $n = 5$) (Fig. 7*C*). However, the application of CGP55845 increased the amplitude of all IPSPs and tended to reduce the IPSPs short-term depression during the train while decreasing the half-width of all EPSPs. On average, the differences between each EPSP1–4 half-peak duration as well as between IPSP1–4 peak amplitudes before and after CGP55845 were significant ($p < 0.05$; paired *t* test; $n = 5$) (Fig. 7*C*). Moreover, the stimulation of the TA path at 5 Hz elicited in CA1 pyramidal cells either stable or slightly facilitating EPSCs at V_H of -70 mV in the presence of 1 μM gabazine ($n = 4$; data not shown). This renders unlikely that the changes observed above were caused by short-term plasticity of monosynaptic TA path-EPSPs recorded in CA1 pyramidal cells. It is also important to note that previous results indicate that high-frequency stimulation of the TA path evokes facilitating excitatory responses in adult interneurons of SLM (Dvorak-Carbone and Schuman, 1999), including juvenile NGFCs (Price et al., 2005). These data, together, suggest that $GABA_B$ receptors expressed by NGFCs dynamically control the excitatory responses from the TA path, most likely affecting the integration time window for TA path-mediated EPSPs converging onto CA1 pyramidal cells.

Discussion

We report here several unique features of the unitary synaptic responses recorded from connected pairs of hippocampal NGFCs of the SLM and CA1 pyramidal cells. Previously, Vida et al. (1998) recorded with sharp microelectrodes uIPSPs from two NGFC–CA1 pyramidal cell pairs. Together with more recent observations in the hippocampus (Fuentealba et al., 2006) and in the neocortex (Tamás et al., 2003), the data indicate that the axon of NGFCs frequently target dendritic shafts and spines of pyramidal neurons. Furthermore, NGFCs form an extensive cellular network with other NGFCs as well as other interneurons of the SLM via chemical and electrical synapses (Price et al., 2005; Zsiros and Maccaferri, 2005; Zsiros et al., 2007). Thus, NGFC is an important example of an interneuron type targeting selectively the distal dendrites of an excitatory neuron.

In our experiments, stimulation of NGFCs evoked $GABA_A$ receptor-mediated uIPSCs with a slow decay in pyramidal cells. Such a slow decay is likely attributable to either the unusually low peak GABA concentration at the synaptic cleft, activation of extrasynaptic $GABA_A$ receptors via GABA spillover, and/or unique structural features of NGFC synapses (Szabadics et al., 2007). Our data thus identify the NGFC type as a source of the slow $GABA_A$ receptor-mediated response recorded from the CA1 hippocampal pyramidal cell (Pearce, 1993). The NGFC also exerts a slow $GABA_A$-receptor response in synaptically coupled NGFCs, in other interneurons of SLM (Price et al., 2005), and in neocortical pyramidal cells (Tamás et al., 2003). The so-called ivy cells also generate slow $GABA_A$ receptor-mediated responses in CA1 pyramidal neurons (Fuentealba et al., 2008). Furthermore, we found that uIPSCs had a small but robust $GABA_B$ receptor-mediated component, consistent with what is observed in hippocampal NGFC–NGFC pairs (Price et al., 2005) and neocortical NGFC–pyramidal cell pairs (Tamás et al., 2003; Szabadics et al., 2007). This is the first time that a unitary $GABA_B$ receptor-mediated response is detected in a GABAergic synapse on a hippocampal excitatory neuron.

Interneurons of the SLM have been proposed to elicit $GABA_B$ receptor-mediated inhibition of CA1 pyramidal cells (Williams and Lacaille, 1992), and our results identify the NGFC as the cell type mediating this slow synaptic response. Our data therefore are complementary to the suggestion that synchronous release of GABA from several interneurons is required to activate $GABA_B$ receptors at hippocampal synapses (Scanziani, 2000; Bertrand and Lacaille, 2001). It is likely that the slow kinetics of synaptic responses mediated by the NGFC–CA1 synapse contributes to

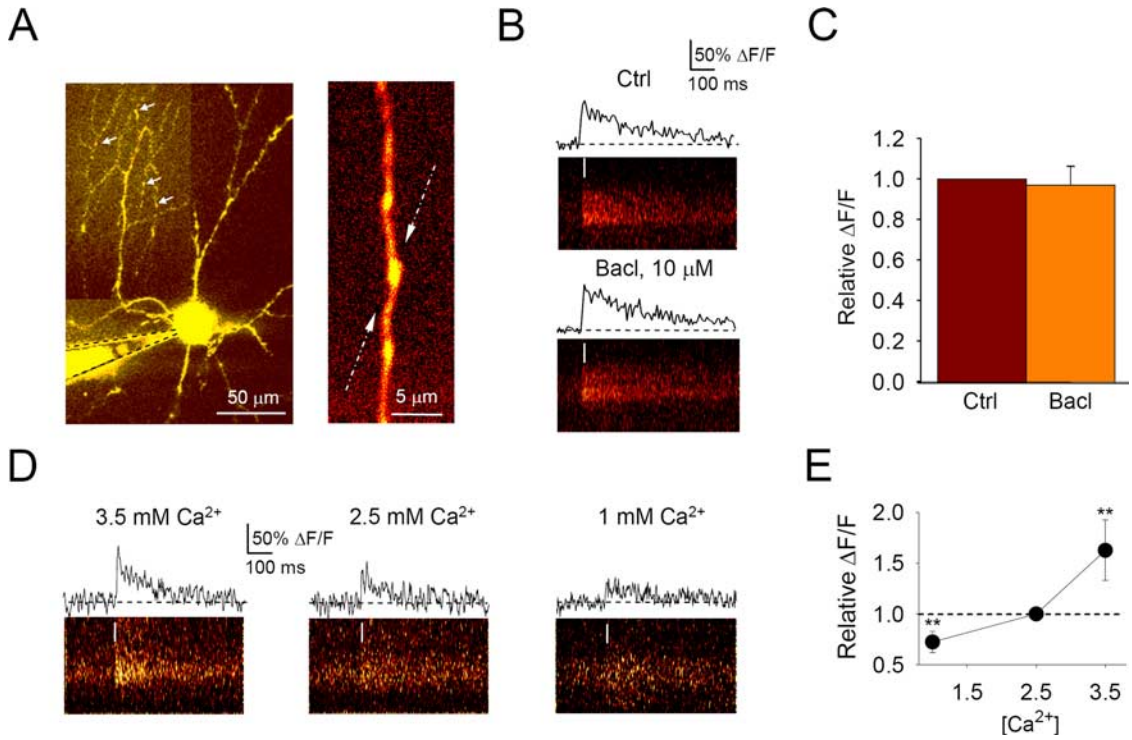

Figure 6. Changing $[Ca^{2+}]_o$, but not the application of baclofen, affects presynaptic Ca^{2+} transients at NGFC axonal boutons. ***A***, Left, Fluorescence image (Alexa channel) of an NGFC (arrows indicate axonal arborization; patch pipette is seen). Right, A characteristic axonal bouton (Alexa channel; arrows, linescan position). ***B***, Ca^{2+}-dependent fluorescent transients (Fluo-4 channel) evoked by single action potentials (white line) in control (Ctrl) and after application of 10 μM baclofen (Bacl). ***C***, Summary; action-potential-evoked $\Delta F/F$ signals were not affected by 10 μM baclofen ($p > 0.70$; paired *t* test; $n = 9$; data are normalized to control). Error bar represents SEM. ***D***, Examples of action potential-evoked presynaptic Ca^{2+}-dependent fluorescent transients (Fluo-4 channel, linescan) under different extracellular Ca^{2+} concentrations, as indicated. ***E***, Normalized pooled data (average and SEM) of the action potential-evoked $\Delta F/F$ signal in the presence of 1, 2.5, and 3.5 mM extracellular Ca^{2+}; the values were significantly different (**$p < 0.01$; ANOVA; $n = 13$).

the prominent theta activity detected in the SLM of hippocampus (Buzsáki, 2002).

Another feature of the NGFC–CA1 pyramidal cell synapse is that it was subjected to presynaptic $GABA_B$ receptor-mediated control similar to that in the hippocampal NGFC–NGFC synapse (Price et al., 2005). The role of tonic presynaptic $GABA_B$ receptor modulation of transmission between other interneuronal types (non-NGFCs) with the soma in the SLM and CA1 pyramidal cells has been debated (Ouardouz and Lacaille, 1997; Bertrand and Lacaille, 2001). We report that action potential-induced Ca^{2+} signals in the dendrites of NGFCs and non-NGFCs decay rapidly with the distance from the soma, consistent with previous reports in other interneuronal types (Kaiser et al., 2001; Goldberg et al., 2003; Topolnik et al., 2006). We found that presynaptic Ca^{2+} transients evoked by the pattern of stimulation that elicited short-term depression in NGFC–CA1 pyramidal cell pairs as well as in NGFC–NGFC pairs (Price et al., 2005) did not significantly change with the application of a $GABA_B$ receptor antagonist. Consistent with this result, baclofen reduced the Ca^{2+} transients in presynaptic boutons of non-NGFCs but not in NGFCs. In contrast, raising or decreasing extracellular Ca^{2+} changed both the amplitude of the uIPSCs and the presynaptic Ca^{2+} transients. It is therefore unlikely that the absence of the effects by the $GABA_B$ receptor ligands on the presynaptic Ca^{2+} signals was caused by a lack of sensitivity of the detection method used. On the contrary, our data argue against the involvement of voltage-dependent Ca^{2+} channels, which are classical targets of presynaptic $GABA_B$ receptors (Takahashi et al., 1998), and against other changes in intraterminal Ca^{2+} dynamics as effectors of $GABA_B$ receptor-mediated actions in NGFCs. One argument against this interpretation is that exocytosis could be triggered by only a few Ca^{2+} channels generating Ca^{2+} nanodomains near a single release site; therefore, the $GABA_B$ receptor-mediated synaptic modulation could be explained by changes in only a few Ca^{2+} channels, which would be undetectable in our experiments. However, this explanation is inconsistent with the stochastic nature of GABA release from multiple release sites at a single synapse (Overstreet and Westbrook, 2003; Telgkamp et al., 2004): if $GABA_B$ receptors were to inhibit Ca^{2+} influx, this should have occurred at all separate release sites. In this case, changes in total Ca^{2+} entry should faithfully reflect changes in the extent of presynaptic Ca^{2+} nanodomains unless the bulk of Ca^{2+} channels are away from the synaptic active zone. The currently available evidence on the subsynaptic distribution of Ca^{2+} channels, the main source of presynaptic Ca^{2+} entry, indicates that the latter is unlikely (Brandt et al., 2005; Kittel et al., 2006). It is therefore highly unlikely that the mechanism in question is confined to local regulation of Ca^{2+} entry among one or a few Ca^{2+} channels and thus cannot be detected. We propose that other mechanisms are involved, including direct modulation of release machinery component(s), which mediates some of the effects of $GABA_B$ receptors at the calyx of Held (Sakaba and Neher, 2003). These mechanisms will require a separate investigation.

What is the role of the $GABA_B$ receptors expressed by NGFCs in the feedforward inhibitory circuit? The TA path connects neurons of layer III of the entorhinal cortex and the apical dendritic tuft of CA1 pyramidal neurons (Witter et al., 1988). This path monosynaptically excites and elicits spikes in the upper apical dendrites of CA1 pyramidal cells, which are propagated to the soma, especially when they occur temporally close to the activa-

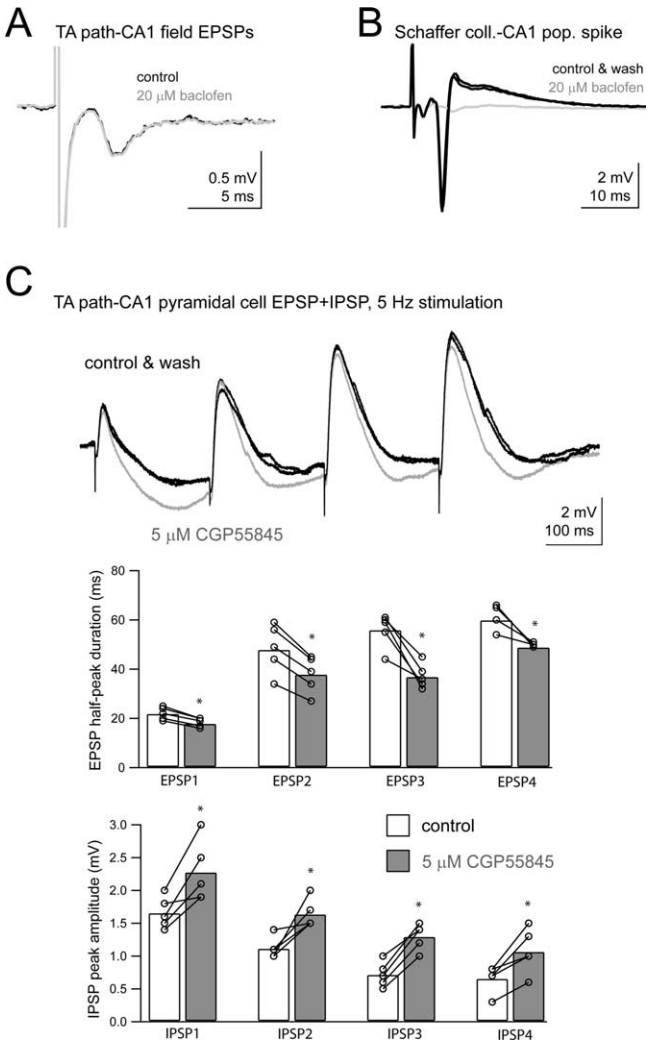

Figure 7. The $GABA_B$ receptors expressed by interneurons of SLM control TA path-mediated feedforward inhibition in CA1 pyramidal cells. ***A***, Presynaptic $GABA_B$ receptors are not functionally expressed by the TA path. The field EPSPs recorded extracellularly in the SLM of CA1 area and evoked by stimulation of the TA path were not changed after the application of the $GABA_B$ receptor agonist baclofen (20 μM, 10 min). ***B***, The Schaffer collateral (coll.)-evoked population spike in CA1 area was greatly reduced by baclofen (20 μM, 6 min), in a reversible manner. Waveforms illustrated in ***A*** and ***B*** are the average of 10 responses; traces are superimposed as indicated. ***C***, Representative traces superimposed in control, in the presence of CGP55845 (5 μM, 10 min), and after washout of CGP55845 (20 min); each trace is the average of three sweeps evoked every 1 min. The voltage responses were recorded in current clamp (resting membrane potential $= -72$ mV) in a CA1 pyramidal cell to four stimuli delivered at 5 Hz to the TA path. In control, note the broadening of the EPSPs evoked after the first stimulus and the gradual decrease of the peak amplitude of the IPSPs during the train stimulation. In the presence of CGP55845, the half-peak duration of the EPSPs was decreased and the IPSP peak amplitude was increased. Pooled data are shown in the top graph (EPSP half-peak duration) and bottom graph (IPSP peak amplitude). All comparisons before and during CGP55845 were statistically significant ($^*p < 0.05$; paired t test; $n = 5$). Data from individual cells are also illustrated (open circles).

tion of the Schaffer-collateral synaptic input, thus resulting in somatic action potential output after distal synaptic stimulation (Jarsky et al., 2005). In addition, the TA path also contacts GABAergic profiles in the SLM (Desmond et al., 1994; Kiss et al., 1996) and excites monosynaptically interneurons with the soma in the SLM (Williams et al., 1994). Among them, the NGFCs are the only interneuronal type known so far to possess both dendritic and axonal arbors segregated within the SLM without sending collaterals to other layers of the CA1 hippocampus, where the dendrites of pyramidal cells are also present (Vida et al., 1998; Price et al., 2005). Therefore, the NGFC is the only major cell type known to provide TA path-mediated feedforward inhibition selectively to the upper apical dendrites of CA1 pyramidal cells. Interestingly, NGFCs are extensively interconnected through gap junctions (Price et al., 2005; Simon et al., 2005; Zsiros and Maccaferri, 2005; Zsiros et al., 2007), which might help to synchronize feedforward inhibition to CA1 pyramidal cells. The TA path–CA1 pyramidal cell synapse is insensitive to $GABA_B$ receptor ligands in normal conditions (Ault and Nadler, 1982; Colbert and Levy, 1992), an observation that we have confirmed here. It is not known whether the $GABA_B$ receptors are expressed at TA path–interneuron synapses, consistent with the target-specific expression of presynaptic receptors at other excitatory synapses (Scanziani et al., 1998). This gave us the chance to analyze selectively the role of $GABA_B$ receptors expressed by NGFCs, and possibly by other interneurons of SLM, on feedforward inhibition. We found that a $GABA_B$ receptor antagonist significantly influenced the dynamic properties of TA path-mediated feedforward inhibition. This suggests that the endogenous activation of $GABA_B$ receptors expressed by NGFCs, as well as possibly by other interneurons of SLM, depresses the release of GABA. In this way, the integration time window of incoming EPSPs and the firing distribution of CA1 pyramidal cells could be modified. Our data complement previous results showing prominent physiological effects by postsynaptic $GABA_B$ receptor-mediated inhibitory responses in CA1 pyramidal cells after TA path stimulation (Dvorak-Carbone and Schuman, 1999).

In several brain circuits, feedforward inhibition limits the temporal summation of EPSPs and generates a narrow "window of excitability" during which action potentials can occur in the postsynaptic neurons (Buzsáki, 1984; Turner, 1990; Pouille and Scanziani, 2001; Blitz and Regehr, 2005; Gabernet et al., 2005; Mittmann et al., 2005). Moreover, feedforward inhibitory circuits are so widespread in the brain (Buzsáki, 1984) and physiologically significant (Swadlow, 2003) that they are likely to be targeted in disease. Indeed, a selective disruption of the feedforward inhibition mediated by the TA path–CA1 circuit occurs in temporal lobe epilepsy (Wozny et al., 2005). Our results showing that $GABA_B$ receptors control the strength of feedforward inhibition in this circuit thus pinpoint a specific receptor that could be targeted for therapeutic intervention.

References

Amaral DG, Witter MP (1995) Hippocampal formation, Ed 2. San Diego: Academic.

Ault B, Nadler JV (1982) Baclofen selectively inhibits transmission at synapses made by axons of CA3 pyramidal cells in the hippocampal slice. J Pharmacol Exp Ther 223:291–297.

Bertrand S, Lacaille JC (2001) Unitary synaptic currents between lacunosum-moleculare interneurones and pyramidal cells in rat hippocampus. J Physiol 532:369–384.

Blitz DM, Regehr WG (2005) Timing and specificity of feed-forward inhibition within the LGN. Neuron 45:917–928.

Brandt A, Khimich D, Moser T (2005) Few CaV1.3 channels regulate the exocytosis of a synaptic vesicle at the hair cell ribbon synapse. J Neurosci 25:11577–11585.

Buzsáki G (1984) Feed-forward inhibition in the hippocampal formation. Prog Neurobiol 22:131–153.

Buzsáki G (2002) Theta oscillations in the hippocampus. Neuron 33:325–340.

Colbert CM, Levy WB (1992) Electrophysiological and pharmacological characterization of perforant path synapses in CA1: mediation by glutamate receptors. J Neurophysiol 68:1–8.

Desmond NL, Scott CA, Jane JA Jr, Levy WB (1994) Ultrastructural identification of entorhinal cortical synapses in CA1 stratum lacunosum-moleculare of the rat. Hippocampus 4:594–600.

Dvorak-Carbone H, Schuman EM (1999) Patterned activity in stratum lacunosum moleculare inhibits CA1 pyramidal neuron firing. J Neurophysiol 82:3213–3222.

Empson RM, Heinemann U (1995a) Perforant path connections to area CA1 are predominantly inhibitory in the rat hippocampal-entorhinal cortex combined slice preparation. Hippocampus 5:104–107.

Empson RM, Heinemann U (1995b) The perforant path projection to hippocampal area CA1 in the rat hippocampal-entorhinal cortex combined slice. J Physiol 484:707–720.

Freund TF, Buzsáki G (1996) Interneurons of the hippocampus. Hippocampus 6:347–470.

Fuentealba P, Klausberger T, Karayannis T, Huck J, Suen W, Studer M, Capogna M, Somogyi P (2006) Firing pattern and synaptic targets of GABAergic neurogliaform cells in the hippocampus in vivo. Paper presented at Fifth Forum of European Neuroscience, Vienna, July.

Fuentealba P, Begum R, Capogna M, Jinno S, Márton LF, Csicsvari J, Thomson A, Somogyi P, Klausberger T (2008) Ivy cells: a population of nitric-oxide-producing, slow-spiking GABAergic neurons and their involvement in hippocampal network activity. Neuron 57:917–929.

Gabernet L, Jadhav SP, Feldman DE, Carandini M, Scanziani M (2005) Somatosensory integration controlled by dynamic thalamocortical feed-forward inhibition. Neuron 48:315–327.

Gähwiler BH, Brown DA (1985) $GABA_B$-receptor-activated K^+ current in voltage-clamped CA3 pyramidal cells in hippocampal cultures. Proc Natl Acad Sci U S A 82:1558–1562.

Gloveli T, Schmitz D, Empson RM, Dugladze T, Heinemann U (1997) Morphological and electrophysiological characterization of layer III cells of the medial entorhinal cortex of the rat. Neuroscience 77:629–648.

Goldberg JH, Tamas G, Yuste R (2003) Ca^{2+} imaging of mouse neocortical interneurone dendrites: Ia-type K^+ channels control action potential backpropagation. J Physiol 551:49–65.

Jarsky T, Roxin A, Kath WL, Spruston N (2005) Conditional dendritic spike propagation following distal synaptic activation of hippocampal CA1 pyramidal neurons. Nat Neurosci 8:1667–1676.

Kaiser KM, Zilberter Y, Sakmann B (2001) Back-propagating action potentials mediate calcium signalling in dendrites of bitufted interneurons in layer 2/3 of rat somatosensory cortex. J Physiol 535:17–31.

Kiss J, Buzsaki G, Morrow JS, Glantz SB, Leranth C (1996) Entorhinal cortical innervation of parvalbumin-containing neurons (Basket and Chandelier cells) in the rat Ammon's horn. Hippocampus 6:239–246.

Kittel RJ, Wichmann C, Rasse TM, Fouquet W, Schmidt M, Schmid A, Wagh DA, Pawlu C, Kellner RR, Willig KI, Hell SW, Buchner E, Heckmann M, Sigrist SJ (2006) Bruchpilot promotes active zone assembly, Ca^{2+} channel clustering, and vesicle release. Science 312:1051–1054.

Maccaferri G, Lacaille JC (2003) Interneuron diversity series: hippocampal interneuron classifications—making things as simple as possible, not simpler. Trends Neurosci 26:564–571.

McBain CJ, Fisahn A (2001) Interneurons unbound. Nat Rev Neurosci 2:11–23.

Mittmann W, Koch U, Hausser M (2005) Feed-forward inhibition shapes the spike output of cerebellar Purkinje cells. J Physiol 563:369–378.

Ouardouz M, Lacaille JC (1997) Properties of unitary IPSCs in hippocampal pyramidal cells originating from different types of interneurons in young rats. J Neurophysiol 77:1939–1949.

Overstreet LS, Westbrook GL (2003) Synapse density regulates independence at unitary inhibitory synapses. J Neurosci 23:2618–2626.

Pearce RA (1993) Physiological evidence for two distinct $GABA_A$ responses in rat hippocampus. Neuron 10:189–200.

Pouille F, Scanziani M (2001) Enforcement of temporal fidelity in pyramidal cells by somatic feed-forward inhibition. Science 293:1159–1163.

Price CJ, Cauli B, Kovacs ER, Kulik A, Lambolez B, Shigemoto R, Capogna M (2005) Neurogliaform neurons form a novel inhibitory network in the hippocampal CA1 area. J Neurosci 25:6775–6786.

Remondes M, Schuman EM (2002) Direct cortical input modulates plasticity and spiking in CA1 pyramidal neurons. Nature 416:736–740.

Rusakov DA, Fine A (2003) Extracellular Ca^{2+} depletion contributes to fast activity-dependent modulation of synaptic transmission in the brain. Neuron 37:287–297.

Rusakov DA, Wuerz A, Kullmann DM (2004) Heterogeneity and specificity of presynaptic Ca^{2+} current modulation by mGluRs at individual hippocampal synapses. Cereb Cortex 14:748–758.

Sakaba T, Neher E (2003) Direct modulation of synaptic vesicle priming by GABA(B) receptor activation at a glutamatergic synapse. Nature 424:775–778.

Scanziani M (2000) GABA spillover activates postsynaptic GABA(B) receptors to control rhythmic hippocampal activity. Neuron 25:673–681.

Scanziani M, Gähwiler BH, Charpak S (1998) Target cell-specific modulation of transmitter release at terminals from a single axon. Proc Natl Acad Sci U S A 95:12004–12009.

Scott R, Rusakov DA (2006) Main determinants of presynaptic Ca^{2+} dynamics at individual mossy fiber–CA3 pyramidal cell synapses. J Neurosci 26:7071–7081.

Simon A, Oláh S, Molnár G, Szabadics J, Tamás G (2005) Gap-junctional coupling between neurogliaform cells and various interneuron types in the neocortex. J Neurosci 25:6278–6285.

Somogyi P, Klausberger T (2005) Defined types of cortical interneurone structure space and spike timing in the hippocampus. J Physiol (Lond) 562:9–26.

Swadlow HA (2003) Fast-spike interneurons and feedforward inhibition in awake sensory neocortex. Cereb Cortex 13:25–32.

Szabadics J, Tamás G, Soltesz I (2007) Different transmitter transients underlie presynaptic cell type specificity of $GABA_{A,slow}$ and $GABA_{A,fast}$. Proc Natl Acad Sci U S A 104:14831–14836.

Takahashi T, Kajikawa Y, Tsujimoto T (1998) G-Protein-coupled modulation of presynaptic calcium currents and transmitter release by a $GABA_B$ receptor. J Neurosci 18:3138–3146.

Tamás G, Lorincz A, Simon A, Szabadics J (2003) Identified sources and targets of slow inhibition in the neocortex. Science 299:1902–1905.

Telgkamp P, Padgett DE, Ledoux VA, Woolley CS, Raman IM (2004) Maintenance of high-frequency transmission at Purkinje to cerebellar nuclear synapses by spillover from boutons with multiple release sites. Neuron 41:113–126.

Thompson SM, Capogna M, Scanziani M (1993) Presynaptic inhibition in the hippocampus. Trends Neurosci 16:222–227.

Topolnik L, Azzi M, Morin F, Kougioumoutzakis A, Lacaille JC (2006) mGluR1/5 subtype-specific calcium signalling and induction of long-term potentiation in rat hippocampal oriens/alveus interneurones. J Physiol 575:115–131.

Turner DA (1990) Feed-forward inhibitory potentials and excitatory interactions in guinea-pig hippocampal pyramidal cells. J Physiol 422:333–350.

Vida I, Halasy K, Szinyei C, Somogyi P, Buhl EH (1998) Unitary IPSPs evoked by interneurons at the stratum radiatum-stratum lacunosum-moleculare border in the CA1 area of the rat hippocampus in vitro. J Physiol 506:755–773.

Vigot R, Barbieri S, Bräuner-Osborne H, Turecek R, Shigemoto R, Zhang YP, Luján R, Jacobson LH, Biermann B, Fritschy JM, Vacher CM, Müller M, Sansig G, Guetg N, Cryan JF, Kaupmann K, Gassmann M, Oertner TG, Bettler B (2006) Differential compartmentalization and distinct functions of GABAB receptor variants. Neuron 50:589–601.

Williams S, Lacaille JC (1992) $GABA_B$ receptor-mediated inhibitory postsynaptic potentials evoked by electrical stimulation and by glutamate stimulation of interneurons in stratum lacunosum-moleculare in hippocampal CA1 pyramidal cells in vitro. Synapse 11:249–258.

Williams S, Samulack DD, Beaulieu C, LaCaille JC (1994) Membrane properties and synaptic: responses of interneurons located near the stratum lacunosum-moleculare/radiatum border of area CA1 in whole-cell recordings from rat hippocampal slices. J Neurophysiol 71:2217–2235.

Witter MP, Griffioen AW, Jorritsma-Byham B, Krijnen JL (1988) Entorhinal projections to the hippocampal CA1 region in the rat: an underestimated pathway. Neurosci Lett 85:193–198.

Wozny C, Gabriel S, Jandova K, Schulze K, Heinemann U, Behr J (2005) Entorhinal cortex entrains epileptiform activity in CA1 in pilocarpine-treated rats. Neurobiol Dis 19:451–460.

Yeckel MF, Berger TW (1990) Feedforward excitation of the hippocampus by afferents from the entorhinal cortex: redefinition of the role of the trisynaptic pathway. Proc Natl Acad Sci U S A 87:5832–5836.

Yeckel MF, Berger TW (1995) Monosynaptic excitation of hippocampal CA1 pyramidal cells by afferents from the entorhinal cortex. Hippocampus 5:108–114.

Zsiros V, Maccaferri G (2005) Electrical coupling between interneurons with different excitable properties in the stratum lacunosum-moleculare of the juvenile CA1 rat hippocampus. J Neurosci 25:8686–8695.

Zsiros V, Aradi I, Maccaferri G (2007) Propagation of postsynaptic currents and potentials via gap junctions in GABAergic networks of the rat hippocampus. J Physiol 578:527–544.

Supplemental figure legends

Supplemental figure 1. **In NGFCs, but not other interneurons of the SLM, the $GABA_B$ receptor ligands CGP55845 or baclofen do not affect Ca^{2+} fluorescent transients elicited by a train of action potentials.** Examples of linescan fluorescent transients in a NGFC (***A1, B1)*** or in a non-NGFC ***(C1)*** axonal boutons evoked by a train of five somatic action potentials at 20 Hz in control (black traces) and in the presence of 5 μm CGP55845 or 10 μM baclofen (red traces). ***A2, B2 and C2***, Average and SEM of fluorescence (ΔF/F) in response to the 1st action potential (1st pulse) and to a train of five action potentials (5 pulses). In NGFC, both data compared to controls were non-significant, $p > 0.70$ paired t-test, n = 7, CGP55845 (***A2***) and n = 10, baclofen (***B2***). Similar experiments in non-NGFC interneurons (n = 9) show depression of action-potential-evoked presynaptic Ca^{2+} signals by baclofen (***C2***); *, $p < 0.03$, ***, $p < 0.001$. ***A3, B3 and C3***, Average and SEM of fluorescence (ΔF/F) in response to each action potential of the train (Pulse number 1-5). In NGFC, all data compared to controls were non-significant, $p > 0.95$, paired t-test, n = 7, CGP55845 (***A3***) and $p > 0.70$ paired t-test, n = 10, baclofen (***B3***). Similar experiments in non-NGFC interneurons (n = 9) show depression of action-potential-evoked presynaptic Ca^{2+} signals by baclofen (***C3***); *, $p < 0.03$, **, $p < 0.01$, ***, $p < 0.001$.

Supplemental figure 2. Baclofen or changes in $[Ca^{2+}]_o$ affect the uIPSCs recorded in CA1 pyramidal cells evoked by a train of action potentials in NGFCs. ***A1,*** *Upper trace*, voltage-clamp recordings (top trace, presynaptic action currents; bottom traces superimposed, average of three sweeps of postsynaptic uIPSCs in control (black trace) and in the presence of 10 μM baclofen (grey trace)) from a NGFC-CA1 pyramidal cell pair showing that baclofen depressed each uIPSCs elicited with the

stimulation at 5 Hz. ***A2,*** The histograms represent the average of each of the four uIPSCs (1-4) recorded during 5 Hz train stimulation under control and baclofen (*, $p < 0.05$, $n = 4$, paired t-test). Data from individual experiments are also shown (empty circles). Whole cell patch clamp recording with cesium-based intracellular solution, V_H of the postsynaptic neurons was -50 mV. ***B1,*** Voltage-clamp recordings (top trace, presynaptic action currents; bottom traces, average of three sweeps of postsynaptic uIPSCs recorded $[Ca^{2+}]_o$ = 3.5 mM, 2.5 mM or 1 mM, as indicated) from a NGFC-CA1 pyramidal cell pair. Each uIPSC elicited with 5 Hz stimulation was affected by changing $[Ca^{2+}]_o$. ***B2,*** The histograms represent the average of each of the four uIPSCs recorded during the stimulation at 5Hz under different $[Ca^{2+}]_o$ (* $p < 0.05$, $n = 4$, ANOVA). Data from individual experiments are also shown (empty circles). Whole cell patch clamp recording with K-gluconate-based intracellular solution, V_H of the postsynaptic neurons was -50 mV.

Supplemental figure 3. The relationship between $[Ca^{2+}]_o$ and presynaptic Ca^{2+} transients in NGFCs.

A, *left,* Fluorescent transients in response to five action potentials at 20 Hz in the presence of 2.5 mM $[Ca^{2+}]_o$ (red trace) and 1 mM $[Ca^{2+}]_o$ (black trace); one cell example. *Right*, Similar experiment but increasing the $[Ca^{2+}]_o$ from 2.5 mM (black trace) to 3.5 mM (red trace). ***B,*** *left,* Summary of experiments shown in A: average normalized amplitude (error bars, SEM) of the ($\Delta F/F$) signal evoked by five action potentials at different $[Ca^{2+}]_o$ (**, $p < 0.01$, $n = 10$, ANOVA). *Right,* Average normalized amplitudes (error bars, SEM) plotted for individual responses to a train of action potentials (**, $p < 0.01$, $n = 10$, ANOVA). ***C,*** *Upper panel,* Ca^{2+} dependent fluorescent transient (Fluo-4 channel) recorded in the bouton shown on the *left* (Alexa

channel) in response to fifty action potentials evoked by somatic depolarizing pulses. *Lower panel,* the application of 100 μM $CdCl_2$ over five minutes abolished the signal. This effect was observed in other two boutons from two different NGFCs.

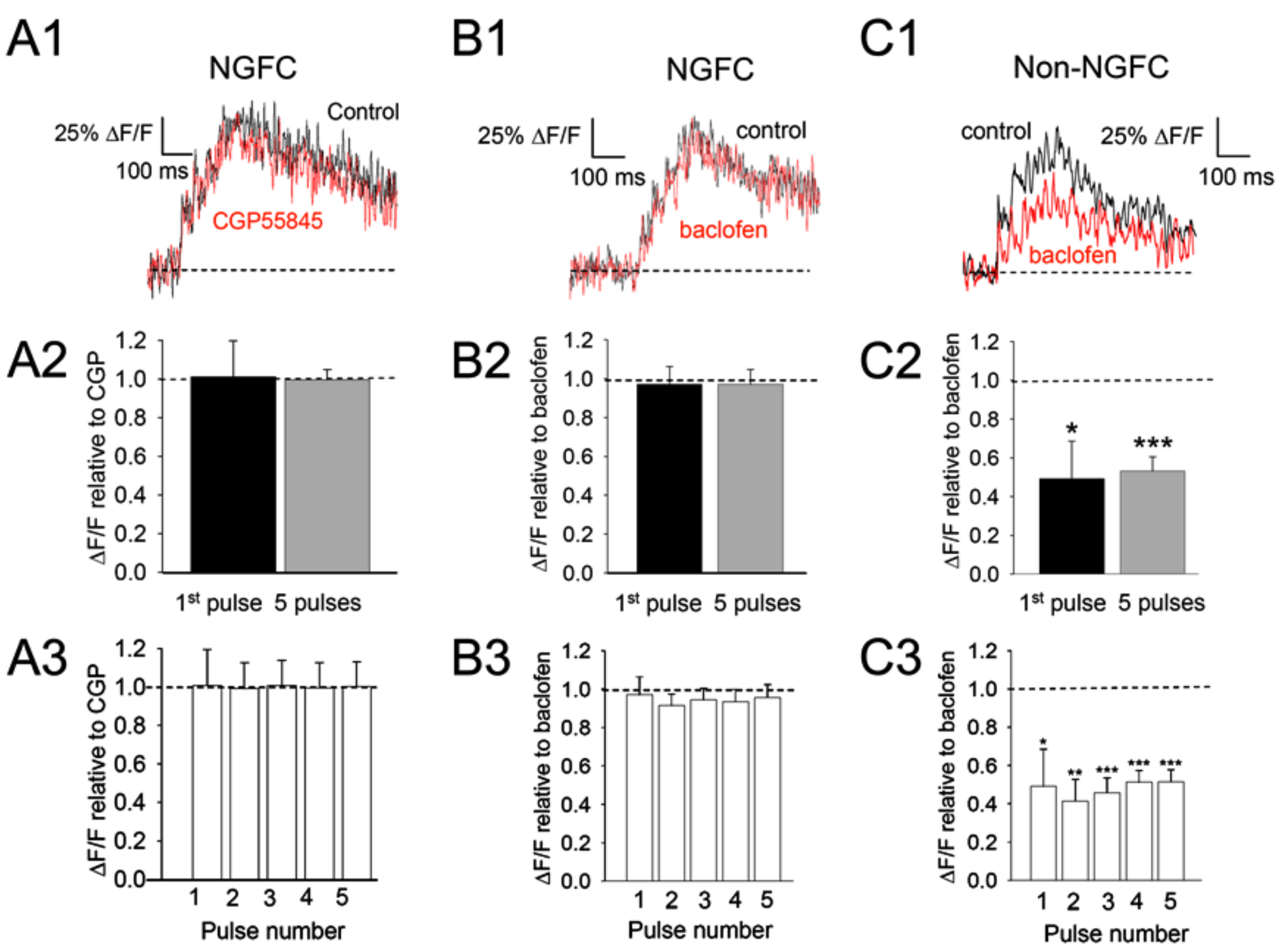
A1
NGFC
25% ΔF/F
100 ms
Control
CGP55845
B1
NGFC
25% ΔF/F
100 ms
control
baclofen
C1
Non-NGFC
control
25% ΔF/F
100 ms
baclofen
A2
ΔF/F relative to CGP
1st pulse 5 pulses
B2
ΔF/F relative to baclofen
1st pulse 5 pulses
C2
ΔF/F relative to baclofen
*
***
1st pulse 5 pulses
A3
ΔF/F relative to CGP
Pulse number
B3
ΔF/F relative to baclofen
Pulse number
C3
ΔF/F relative to baclofen
*
**
***
***
***
Pulse number

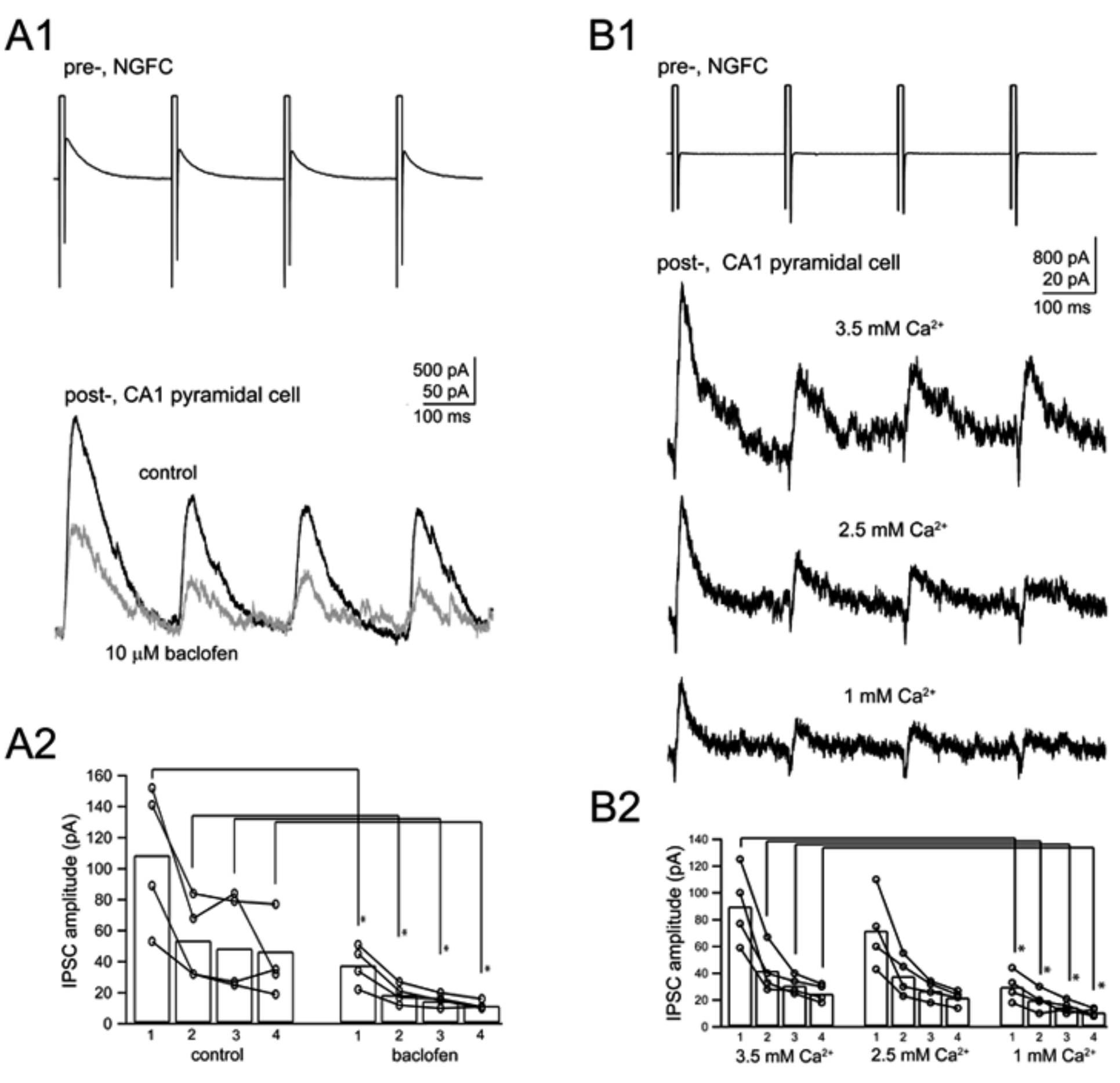
A1
pre-, NGFC
post-, CA1 pyramidal cell
500 pA
50 pA
100 ms
control
10 μM baclofen
A2
IPSC amplitude (pA)
control
baclofen
B1
pre-, NGFC
post-, CA1 pyramidal cell
800 pA
20 pA
100 ms
3.5 mM Ca2+
2.5 mM Ca2+
1 mM Ca2+
B2
IPSC amplitude (pA)
3.5 mM Ca2+
2.5 mM Ca2+
1 mM Ca2+

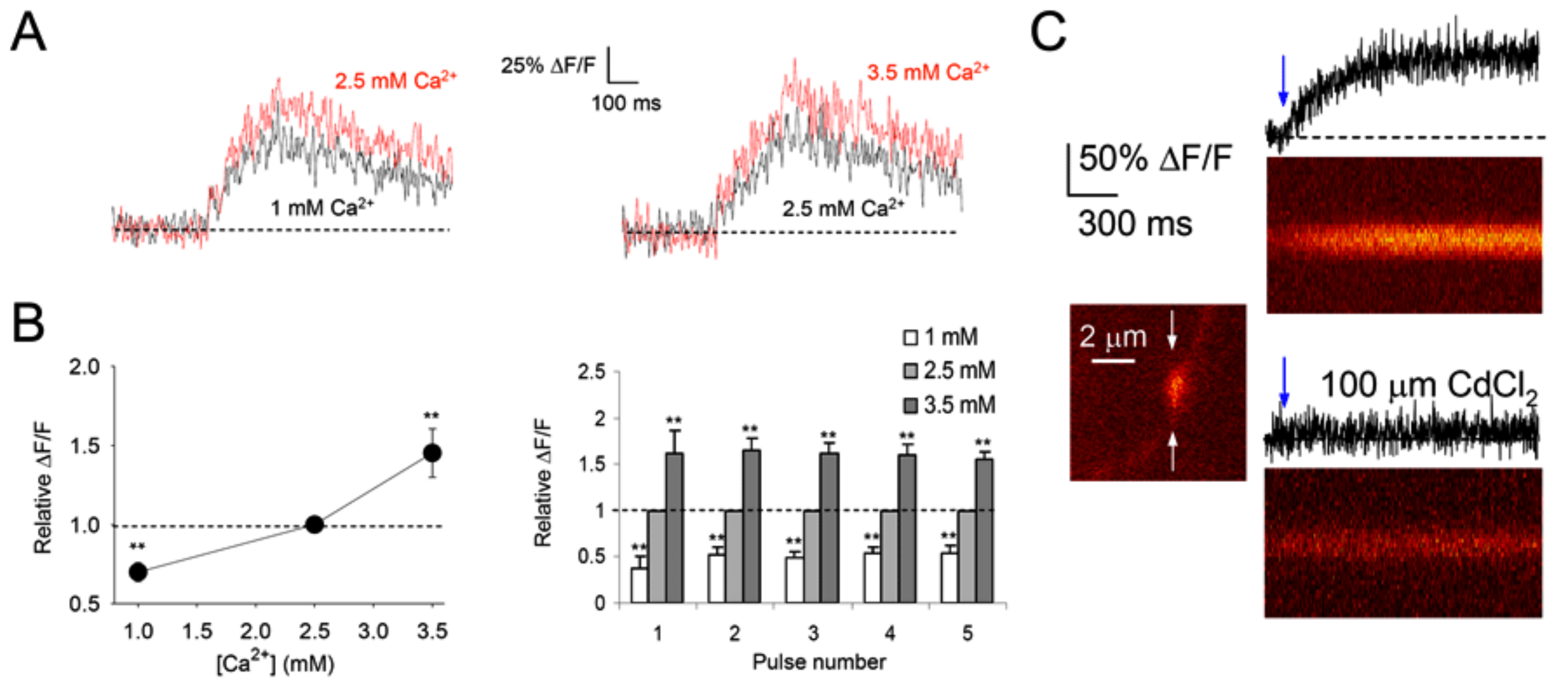
A
2.5 mM Ca2+
1 mM Ca2+
25% ΔF/F
100 ms
3.5 mM Ca2+
2.5 mM Ca2+
B
Relative ΔF/F
[Ca2+] (mM)
1 mM
2.5 mM
3.5 mM
Pulse number
C
50% ΔF/F
300 ms
2 μm
100 μm CdCl2